



HAL
open science

Some examples of the use of structure functions in the analysis of satellite images of the ocean

Lucien Wald

► **To cite this version:**

Lucien Wald. Some examples of the use of structure functions in the analysis of satellite images of the ocean. Photogrammetric engineering and remote sensing, 1983, 55, pp.1487-1490. hal-00464058

HAL Id: hal-00464058

<https://minesparis-psl.hal.science/hal-00464058>

Submitted on 16 Mar 2010

HAL is a multi-disciplinary open access archive for the deposit and dissemination of scientific research documents, whether they are published or not. The documents may come from teaching and research institutions in France or abroad, or from public or private research centers.

L'archive ouverte pluridisciplinaire **HAL**, est destinée au dépôt et à la diffusion de documents scientifiques de niveau recherche, publiés ou non, émanant des établissements d'enseignement et de recherche français ou étrangers, des laboratoires publics ou privés.

Some Examples of the Use of Structure Functions in the Analysis of Satellite Images of the Ocean

L. Wald

Centre de Télédétection et d'Analyse des Milieux Naturels, Ecole Nationale Supérieure des Mines de Paris, Sophia-Antipolis, 06565 Valbonne, France

ABSTRACT: This paper deals with the use of the structure function, also called a variogram, to analyze satellite images of the ocean. The structure function is a powerful tool for the description of two-dimensional random fields. Its characteristics are used in two different examples. First, the behavior of the structure function close to its origin gives the variance of salt and pepper noise within an image. Such a method has been applied to various spaceborne sensors. Second, fitting the experimental structure function by a power law demonstrates the way the turbulent energy at the surface of the ocean is transferred from scales to scales.

INTRODUCTION TO THE STRUCTURE FUNCTION OR VARIOGRAM

LET US DEFINE the two-dimensional space variable as x . Following Matheron (1963, 1970a, 1970b, 1973), we interpret a two-dimensional field data set as samples of a non-stationary random function $Z(x)$. If $Z(x)$ has stationary increments and for a distance h , the structure function or variogram, D , has the expected value

$$D_{zz}(h) = E((Z(x+h) - Z(x))^2) \quad (1)$$

This quantity divided by two is called a semivariogram or intrinsic function and has been, and still is, widely used in geology, in particular, mining (see, e.g., Matheron (1963) and Royle (1980) among many others). The structure function itself has been successfully used for some time in the study of the structure of turbulent fields in the atmosphere and the ocean (see, e.g., Kolmogorov (1941) or Panchev (1971) or Gage (1979)). It has also been used in digital imagery (Serra, 1982) and also in remote sensing to filter out noise in images (Albuissou, 1976) or to explore Landsat data (Carry and Myers, 1984) or to analyze texture as an aid to the classification of multispectral data (Sarrat, 1977), among many other uses.

The structure function depicts the spatial variability at increasing distances (scales) between sample points. It puts on a rational and numerical basis the well-known concept of the "range of influence" of the variable in a fashion more or less similar to the covariance function for a stationary function. It also gives a measure of the variance of the structures the sizes of which are smaller than the sampling size. This variance is called the nugget effect or nugget variance or random variance as shown in Figure 1, which illustrates a typical structure function. The spatial behavior of $Z(x)$ is closely related to the shape of $D_{zz}(h)$ near the origin. If $D_{zz}(h)$ is twice differentiable at the origin, then $Z(x)$ is smoothly continuous and it contains rather energetic long wavelength terms. If $D_{zz}(h)$ is linear near the origin, then $Z(x)$ is continuous but not necessarily derivable. If $D_{zz}(h)$ is not continuous at the origin, hence presenting a nugget effect, $Z(x)$ is not continuous and is rather erratic.

The structure function may be linked to the widely known and used Fourier transform. For a second-order stationary random function, the structure function may be expressed as a function of the covariance $B(h)$: i.e.,

$$D_{zz}(h) / 2 = B(0) - B(h) \quad (2)$$

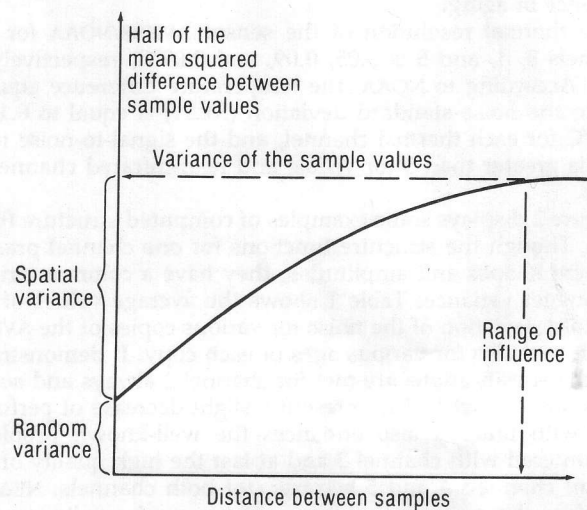


FIG. 1. A typical semivariogram. (Royle, 1980).

If \mathcal{F} means the Fourier transform and if $E(k)$ is the spectral density of variance, k being the wavevector, it follows (Panchev, 1971) that

$$D_{zz}(h) / 2 = \int E(k) dk - \mathcal{F}^{-1}(E(k)). \quad (3)$$

As an example, if $E(k) \sim k^{-n}$, with $n > 1$, $D(h) \sim h^{n-1}$. The spectrum $E(k)$ of a periodic function $Z(x)$ will display peaks and $D_{zz}(h)$ a series of bumps, both denoting the period (fundamental plus harmonics). However, the Fourier transform is better than the structure function to show up periodic phenomena because peaks offer a better determination of the periods than do bumps.

Some of the characteristics of the behavior of the structure function are now used in two examples. First, the nugget effect is used to provide the variance of salt and pepper noise present in satellite imagery. Second, the way the turbulent energy cascades from scales to scales at the surface of the ocean is examined by fitting a power law onto experimental structure functions. Regarding the calculation of the structure function by a computer, it can be done either in the direct way (Equation

1), which takes a lot CPU time or by using a Fast Fourier Transform routine and applying Equation 3.

ESTIMATING SALT AND PEPPER NOISE IN IMAGERY

Salt and pepper noise characterizes the scattering of the radiometric measurements for a same impinging signal. Given an image it is usually estimated by the use of the Fourier transform (Jenkins and Watts, 1969; Oppenheim and Schaffer, 1975). However, the very chaotic behavior of the spectral density for high wavenumbers as well as the presence of large scale trends may render the estimates rather inaccurate. Because the variance of the noise appears in the structure function as the nugget variance, structure function offer a good readiness of the noise variance even in presence of large variations of the actual signal. It is also invariant, by definition, to systematic errors.

Two examples are now given regarding the Advanced Very High Resolution Radiometer (AVHRR) aboard the NOAA satellite series and the Coastal Color Zone Scanner (CZCS) aboard the Nimbus 7 satellite. First, the structure functions are computed from images containing raw data. Second, the noise variance is estimated and is compared to the prior-to-flight specifications of the sensor. Third, operations are repeated to examine the influence of aging.

The thermal resolution of the sensor AVHRR/NOAA for the channels 3, 4, and 5 is 0.05, 0.09, and 0.09°C, respectively at 23°C. According to NOAA, the temperature difference equivalent to the noise standard deviation (NEAT) is equal to 0.12°C at 23°C for each thermal channel, and the signal-to-noise ratio (S/N) is greater than 3 for visible and near-infrared channels 1 and 2.

Figure 2 displays some examples of computed structure functions. Though the structure functions for one channel present different shapes and amplitudes, they have a common origin: the nugget variance. Table 1 shows the average values of the standard deviation of the noise for various copies of the AVHRR sensor and also for various ages of each copy. It demonstrates that the specifications are met for channel 2 always and sometimes for channel 1. Both present a slight decrease of performance with time. It also enhances the well-known problems encountered with channel 3 and at last the high quality of the data of channels 4 and 5 because, for both channels, NEAT is less than the resolution (0.09°C). These good results are also stable with time.

In the same fashion the salt and pepper noise present in the raw images provided by the CZCS aboard Nimbus 7 has been estimated. The four possible values of gain were taken into account. Table 2 shows mean values of the signal-to-noise ratio as a function of channel and time. These values are in agreement with the sensor specifications of NASA except for thermal

channel 6 which is rather noisy. Table 2 demonstrates a decrease of performance with time except for channel 5. This decrease is not constant in time, and sensor noise was higher during 1981 than 1982, except for channels 4 and 6.

THERMAL IMAGERY AND OCEANIC TURBULENCE

Statistical analyses of the mesoscale temperature field are of primary interest for the comprehension of oceanic turbulence. For such a turbulent field, the structure function is quite smooth because all scales are present within an image, none of them being predominant. It may be fitted by a power law, the exponent of which indicates, briefly speaking, how the energy transfers from scales to scales. The turbulent part of infrared images from both the sensor VHRR/NOAA-5 and the sensor HCMR/AEM-1 was investigated by Deschamps *et al.* (1981) and Wald (1980). Structure functions were computed (Figure 3) and a power law was fitted to each of them. Their results show that the structure function $D_{TT}(\mathbf{h})$ of the thermal turbulent field can be accurately described by a power law within the range of scales 3 to 100 km: i.e.,

$$D_{TT}(\mathbf{h}) = D_{TT}(h, \Theta) = A(\Theta) h^{n-1} \quad (4)$$

where h is the scale and Θ the polar angle of the vector \mathbf{h} . The anisotropy of the temperature field appears only in the amplitude of the structure function while the exponent is isotropic. In the stationary case, to this structure function there corresponds a temperature variance spectral density: i.e.,

$$E_T(k, \Theta) = C(\Theta) k^{-n}. \quad (5)$$

The value of n ranges between 1.5 and 2.3 with a mean value of 1.8. Similar results were found either from airborne measurements (Saunders, 1972; Liu and Katsaros, 1984) or from ship towed sensor (Fieux *et al.*, 1978). These results are in very good agreement with the theory of Blumen (1978) which deals with quasi-geostrophic turbulence at the surface of the ocean. It assumes the conservation of both the total energy of the system and the potential energy at the surface. These hypotheses imply a cascade of the latter towards the greatest wavenumbers. The spectral density of the available potential energy is a power law of the horizontal wavenumber k whose exponent is equal to $-5/3$ (~ -1.67). The spectral density of the variance of a passive scalar follows a similar law (Lesieur and Sadourny, 1981) and so does the temperature variance spectral density.

The influence of atmospheric effects upon the exponent has only been partly addressed by the above cited authors. The radiometric temperature T_B measured from space can be expressed by the now usual form:

$$T_B = t T + T_A \quad (6)$$

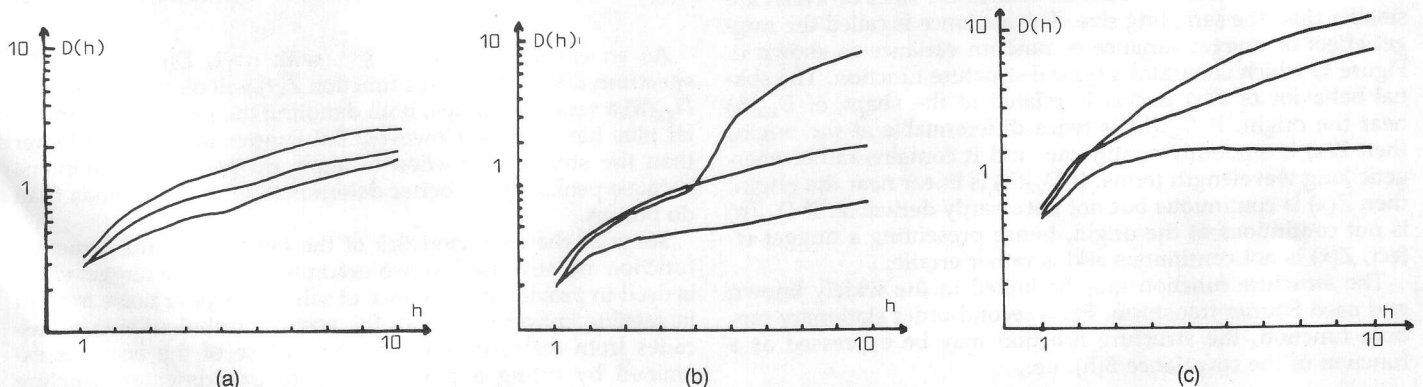


FIG. 2. Some examples of structure functions computed from various AVHRR/NOAA images to estimate the salt and pepper noise. (a) channel 1 (VIS), (b) channel 2 (NIR), (c) channel 5 (IR).

TABLE 1. ESTIMATES OF THE AVHRR/NOAA NOISE. VALUES ARE SIGNAL-TO-NOISE RATIO FOR CHANNELS 1 AND 2 AND NEAT (°C) FOR CHANNELS 3 TO 5.

Satellite Age (year)	NOAA 6		NOAA 7		NOAA 8	NOAA spec.
	1.5	5	2	3	1	
VIS 1	2.6	2.8	2.3	3.0	2.8	>3
NIR 2	3.3	4.0	2.6	3.5	2.9	>3
IR 3	0.06	0.13	0.11	0.38	0.42	0.12
IR 4	0.06	0.06	0.04	0.04	0.05	0.12
IR 5	0.06	0.06	0.05	0.05	0.05	0.12

TABLE 2. ESTIMATES OF THE NOISE FOR THE SIX CHANNELS OF THE CZCS/NIMBUS 7

Year	1979	1980	1981	1982	1983	NASA spec.
1 (S/N)	276	268	211	218	197	> 150
2 (S/N)	289	277	201	201	191	> 140
3 (S/N)	256	243	174	192	159	> 125
4 (S/N)	148	131	126	123	112	> 100
5 (S/N)	241	248	239	284	248	> 100
6 (°C)	0.28	0.28	0.28	0.30	0.57	0.22

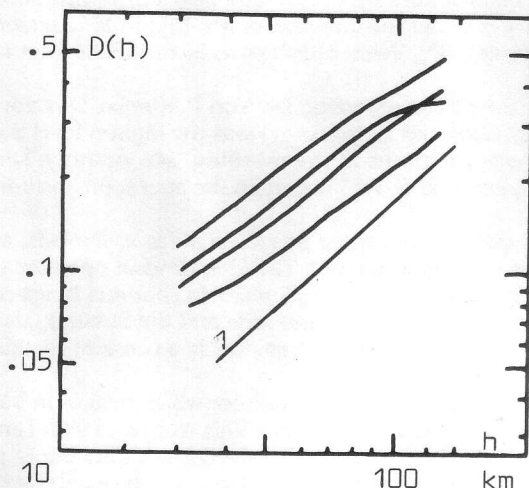


FIG. 3. An example of structure function computed from a VHRR/NOAA-5 image of the sea surface temperature field showing the continuity of scales present in mesoscale turbulent structures. (Wald, 1980).

where T is the water temperature, t the atmospheric transmittance, and T_A an appropriate mean air temperature. The structure function of the water temperature is, therefore, a combination of unknown structure functions of products and of cross-structure functions involving the three parameters T , t , and T_A . The above cited authors assume that the atmospheric parameters, t and T_A , are stable within the scale range 1 to 100 km. Hence, they can write

$$D_{TtB}(h) = t^2 D_{TT}(h) \quad (7)$$

where the influence of the atmosphere affects only the determination of the structure function amplitude and not the determination of the exponent. But this assumption is not valid because these parameters present also spatial fluctuations within this range. Like the others atmospheric passive scalars, their spectra follow a power law whose exponent is $-5/3$ (see a review, e.g., in Gage (1979) or Panchev (1971)). Hence, the influence of

the atmosphere may be suspected in their results. However, this influence of these parameters is lessened by the high level of salt and pepper noise present in the VHRR images used, whose temperature difference equivalent to the noise standard deviation (NEAT) was found to be 0.7 to 0.8°C for a radiometric accuracy of 0.5°C (Wald, 1980). It follows that, for the clear atmospheres under consideration, the fluctuations of the atmospheric parameters and their relative importance were small enough not to induce sensible changes in the variations of T , and hence that the results of Deschamps *et al.* and Wald are still valid.

Some of the images were also analyzed by a direct computation of the spectral density of the temperature variance. Of course, similar results were obtained. However, the structure function was preferred for the following reasons. The readiness of a structure function is better than one of a spectral density and, far from the origin, the fitting of a power law onto the structure function offers a better determination of the exponent than does a spectral density. Also, structure functions are insensitive to systematic changes or errors while spectra are not. These systematic changes may be related, for example, to the atmospheric effects on the signal upwelling from the sea. Hence, once the nugget effect is subtracted, structure functions may be compared to each other.

CONCLUSION

Two examples have been presented of the use of the structure function or variogram to analyze satellite images of the ocean. The structure function is a powerful tool for the description of two-dimensional random fields. Its characteristics have been proven accurate estimates of some oceanic parameters. The first example given here can be extended to other sensors to obtain the level of the salt and pepper noise which effects the accuracy of the final results. Also, statistical analyses using structure functions may be applied to other ocean variables. Beyond their interest in the comprehension of the oceanic turbulence, such analyses offer means in numerical modeling for the parametrization of the unresolved motions or submesh phenomena.

REFERENCES

- Albuissou, M., 1976. *Analyse de texture et lissage optimal des images thermographiques par satellite*. Thèse de 3ème cycle, Institut de Statistique des Universités de Paris, France.
- Blumen, W., 1978. Uniform potential vorticity flow. Part 1: Theory of wave interactions and two-dimensional turbulence, *J. Atmos. Sci.* 35, 774-783.
- Carr, J.R., and D.E. Myers, 1984. Application of the theory of regionalized variables to the spatial analysis of Landsat data, *Proceedings of the Pecora 9 Spatial Information Technologies for Remote Sensing Today and Tomorrow*, IEEE Computer Society Press, pp. 55-61.
- Deschamps, P.Y., R. Frouin and L. Wald, 1981. Satellite determination of the mesoscale variability of the sea surface temperature, *J. Phys. Oceanogr.*, 11, 6, 864-870.
- Fieux, M., S. Garzoli and J. Gonella, 1978. Contribution à la connaissance de la structure spatiale des courants superficiels au large du Golfe du Lion, *J. Rech. Océanogr.*, 3, 4, 13-26.
- Gage, K.S., 1979. Evidence for a $k^{-5/3}$ law inertial range in mesoscale two-dimensional turbulence, *J. Atmos. Sci.* 36, 1950-1954.
- Jenkins, G.M. and D.G. Watts, 1969. *Spectral Analysis and its Applications*, Holden-Day, San Francisco, 525p.
- Kolmogorov, A.N., 1941. The local structure of turbulence in incompressible viscous fluid for very large Reynolds numbers. *Dokl. Akad. Nauk. SSSR*, 30, 301-305.
- Lesieur, M., and R. Sadourny, 1981. Satellite-sensed turbulent ocean structure, *Nature*, 294, 673.
- Liu, W.T., and K.B. Katsaros, 1984. Spatial variations of sea surface temperature and flux-related parameters measured from an aircraft in the JASIN experiment, *J. Geophys. Res.*, 89, C6, 10651-10644.

- Matheron, G., 1963. Principles of Geostatistics, *Economic Geology*, 58, 1246-1266.
- , 1970a. *La théorie des variables régionalisées et ses applications*, Cahiers du Centre de Morphologie Mathématique, Ecole Nationale Supérieure des Mines de Paris, 212 p.
- , 1970b. Random functions and their application in geology, *Geostatistics, a Colloquium*, (D.F. Merriam, ed.), Plenum Publ. Co, New York. pp. 79-88.
- , 1973. The intrinsic random functions and their applications, *Advances in Applied Probability*, 5, 439-468.
- Oppenheim, A.V., and R.W. Schaffer, 1975. *Digital Signal Processing*, Prentice-Hall Inc., Englewood Cliffs, New Jersey, 608 p.
- Panchev, S., 1971. *Random Functions and Turbulence*, Pergamon Press, 444 p.
- Royle, A.G., 1980. Why Geostatistics?, *Geostatistics*, McGraw-Hill, New York, pp. 1-16.
- Sarrat, D., 1977. *Analyse de la texture des images de réflectance terrestre*. Thèse de 3ème cycle, Université Paul Sabatier, Toulouse, France.
- Serra, J., 1982. *Image Analysis and Mathematical Morphology*, Academic Press, London, 610p.
- Saunders, P.M., 1972. Space and time variability of temperature in the upper ocean, *Deep-Sea Res.*, 19, 467-480.
- Wald L., 1980. *Utilisation du satellite NOAA-5 à la connaissance de la thermique océanique. Etude de ses variations saisonnières en mer Ligure et de ses variations spatiales en Méditerranée*. Thèse de 3ème Cycle, Université Paris VI, Paris, France.

(Received 29 November 1988; accepted 23 February 1989; revised 22 March 1989)

SOVIET SATELLITE IMAGING AND IMAGE TECHNOLOGY SEMINAR

The National Geographic Society hosted a seminar on Soviet satellite remote sensing on June 21, 1989. A Soviet foreign trade association (SOJUZKARTA) has been recently created in the spirit of glasnost to release and distribute imagery from several of the Soviet space programs. Soviet imagery is being marketed in the Western Hemisphere by ContiTrade Services Corporation, a subsidiary of Continental Grain Company. Marketing of the Soviet space imagery is under the direction of Mr. Myron R. Laserson, Senior Marketing Director of ContiTrade. ContiTrade in turn has employed the services of Dr. Velon Minshew as its resident expert in remote sensing technology and applications.

Mr. Laserson gave the opening remarks at the seminar, and Dr. Minshew served as moderator. Dr. Yuri P. Kienko, Director General of PRIRODA (the Soviet state scientific research and production center for geodesy and cartography) was the highest level Soviet official at the seminar, and presented the technical aspects of the Soviet space programs in the morning. Mr. Anatoly, Director of Kosmokarta (one of the SOJUZKARTA firms) presented the some of the applications of the imagery in the afternoon, including those in the developing countries.

ContiTrade had used three U.S. image processing firms to digitally scan many Soviet space images of areas in the U.S., and these firms supplied the exhibits and scientists who presented their results to the seminar attendees. The U.S. Landsat operator (EOSAT) and the French SPOT-Image Company also provided personnel who spoke about their country's plans to continue in space remote sensing commercialization. The exhibits were displayed around the lunch tables (hosted by ContiTrade and the Soviets), and interactive PC-based digital systems were installed around the balcony over the attendees' heads as they ate lunch, a constant reminder to go see them when they were finished eating.

The Soviets are releasing photographs from the multispectral MK-4 camera and the KFA-1000 camera which images in both black-and-white, and color. The MK-4 images with a ground resolution of 6 meters, the KFA-1000 5 meters. This compares with Landsat's 30 meter resolution and SPOT's 10 meter (black-and-white) and 20 meter (color). The Soviets at the present sell only photo products. Both cameras sense on film, hence no digital tapes are available. (SOJUZKARTA promises that digital tapes will be available next year, and will be formatted to be compatible with the Landsat and SPOT tapes). ContiTrade is promoting the digitization of the photos for analysis and display.

The Soviets will not sell data of their country, any East Bloc state, or any of the communist or Marxist developing countries. When asked whether the Soviets were planning to abide by the U.N. "open skies" policy; i.e., the open nondiscriminatory distribution of imagery data to all nations of the world, Dr. Kienko replied that the Soviets would abide by all U.N. resolutions. Since there exists a U.N. resolution regarding space operators providing all civil satellite remote sensing data to everyone, it is difficult to see how the Soviets resolve their agreement to abide by U.N. resolutions and at the same time restrict data taken over communist-based regimes.

The Soviets said little about the impacts that space imagery was having on key environmental problems in their country. When asked why ContiTrade was restricted from selling Soviet photography in Argentina, Brazil, and Peru (in addition to the obvious restrictions in Cuba and Nicaragua), the reply was that the Soviets had long histories of cooperation in space remote sensing in these three countries as well. The Soviets seem to have no misgivings about Soviet imagery and Western remote sensing data sources (Landsat and SPOT) being used together in projects in developing countries such as Peru.

—C.K. Paul